Journal of Power Sources, *12* (1984) 289 - 303

DEGRADATION IN NICKEL–CADMIUM CELLS STUDIED BY IMPEDANCE MEASUREMENTS

RON HAAK, CAMERON OGDEN and DENNIS TENCH
Rockwell International Science Center, Thousand Oaks, CA 91360 (U S A)
SAL DI STEFANO
Jet Propulsion Laboratory, Pasadena, California (U S A)

Summary

The impedance of 12 A h Ni–Cd sealed cells was evaluated as a nondestructive, *in situ* means of determining cell lifetime, particularly with respect to the probability of premature failure The Ni–Cd cell impedance was measured (10 000 to 0.0004 Hz) as cells were subjected to charge/discharge cycle testing under a variety of temperature and depth-of-discharge conditions

The results indicate that cell degradation is reflected in the low frequency impedance characteristics associated with diffusional processes. The slope (W) of the low frequency portion of complex plane impedance plots obtained from totally discharged Ni–Cd cells was found to increase with charge/discharge cycling In addition, based on data for two cells, a high or rapidly increasing W value signals imminent cell failure by one mechanism. Degradation by another mechanism is apparently reflected in a fall-off of the imaginary impedance component at low frequencies.

The frequency dependence of the absolute cell impedance at low frequencies (0.5 - 0.005 Hz) was found to vary monotonically with cell state-of-charge.

Introduction

Especially for aerospace applications, a nondestructive means of detecting flaws in batteries and predicting cycle life is needed so that costly, and sometimes dangerous, premature failures can be avoided. Cell impedance characteristics determined over a wide frequency range should be sensitive to imperfections in both the electrode and separator materials and, thus, could provide the desired information.

Impedance characteristics of a number of commercial battery systems have been investigated, typically with the goal of developing a method for determining the state-of-charge. Hampson *et al.* [1] have reviewed the literature prior to 1979 and report a general theory for describing the impedance of batteries. Systems that have been studied include Zn/HgO

0378-7753/84/$3 00

[2, 3], Zn/MnO_2 [4, 5], Leclanché cells [6 - 8], Pb/H_2SO_4 [9 - 11], Mg/MnO_2 [5] and Ni–Cd [12 - 14]. The effects of charge/discharge cycling on Pb [15], sintered-plate Cd electrodes [16], and Ni–Cd cells [14] have been investigated. These studies, although not particularly successful in establishing state-of-charge correlations, have demonstrated the value of impedance measurements for investigation of battery properties.

Zimmerman *et al* [12] determined that the impedance of an operating Ni–Cd battery is dominated by mass transport processes. Two diffusional features were observed in the impedance spectra one apparently corresponding to solid state proton diffusion within the nickel oxy-hydroxide electrode and the other to cadmium diffusion. Zimmerman and co-workers note that the diffusional processes in Ni–Cd cells are sensitive to changes in the morphology or chemical structure of the electrode active material. In a recent study, Zimmerman and Janecki [14] report that the voltage losses that occur in Ni–Cd cells during charge/discharge cycling are accompanied by changes in the Ni electrode impedance and probably involve separation of β-NiOOH and γ-NiOOH phases Sathyanarayana *et al* [13] conclude that the impedance of Ni–Cd cells is dominated by diffusion and may be interpreted in terms of a long, cylindrical pore model. The latter authors found that the equivalent series and parallel capacitance reflect (within 20 - 30%) the battery state-of-charge

Interpretation of impedance data for commercial Ni–Cd cells presents a challenge since the cell is typically sealed so that the contributions of the individual electrodes and electrolyte/separator must be inferred from the total cell impedance The situation is further complicated by the porous nature of the electrode

Impedance characteristics of porous electrodes have been treated theoretically by de Levie [17], using a transmission line model and assuming infinitely-deep, cylindrical pores of uniform cross section. Whereas interfacial impedances are simply additive for a planar surface, they combine as the geometric mean for such porous electrodes. Consequently, impedance characteristics for a given process may be significantly affected by the electrode porosity. For example, whereas the diffusional impedance for a planar electrode is directly proportional to $\omega^{-1/2}$ ($\omega = 2\pi f$, f = perturbation frequency in Hz), it is proportional to $\omega^{-1/4}$ for porous electrodes of the type treated by de Levie. For electrodes having such idealized pores, the impedance can be correlated with that for planar electrodes by squaring the absolute magnitude of the impedance and doubling the phase angle [17].

For real porous electrode systems, nonidealized behavior must also be considered For example, since at lower perturbation frequencies pores must be deeper to behave as though infinitely deep, a transition from porous to nonporous electrode behavior can occur as ω is changed over a few decades [17] Thus, for a typical frequency scan, which covers seven decades (*e g*, 10 kHz - 1 mHz), it is quite possible to encounter both porous and nonporous behavior This has been used to advantage by Armstrong *et al* [16], who were able to detect a decrease in pore length for Cd electrodes in

alkaline solution caused by redistribution of active material and a progressive buildup of $Cd(OH)_2$ during charge/discharge cycling The effect of pore geometry on impedance spectra has been addressed by Keiser *et al* [18], noncylindrical pores, especially those with occluded geometries, were shown to exhibit anomalous impedance behavior. These authors were able to discern the average pore structure of a nickel electrode from impedance measurements.

In the present study, the impedance characteristics of a relatively large number of Ni–Cd cells were determined at various times in an accelerated charge/discharge testing program and were empirically examined for features which could be easily identified and cataloged for later correlation with cell lifetime and cycle history Emphasis was on developing impedance characterization as a quality control technique, which could be applied and interpreted in a straightforward manner rather than on interpretation of the data in an absolute sense.

Experimental

Testing was performed on 12 A h sealed cells (General Electric) for which the Ni active material was either chemically (L2 series) or electrochemically (L1 series) deposited. The charge/discharge cycle was based on a satellite low earth orbit and consisted of 60 min charging and 40 min discharging. Nine test conditions were used, defined by the matrix of three temperatures (20, 30 and 40 °C) and three depths of discharge (20, 35 and 50%). Statistical information is available for the average cycle life under a given set of conditions; for example, at 40 °C and 50% depth of discharge, cells have a 63% chance of failing by 3100 cycles [19]

Impedance measurements were performed under potentiostatic control using a Solartron Model 1172 frequency response analyzer, which determines the real and imaginary components of the impedance, in conjunction with a Stonehart Model BC 1200 potentiostat. The Stonehart potentiostat has the advantage of dual reference inputs, which minimize lead wire inductive effects. The voltage perturbation used in the present work was 2 mV (rms), except for preliminary studies (10 mV). Impedance was measured from 10 kHz to about 0.4 mHz, with 20 logarithmically-spaced points per decade of frequency. Full computer control of the experiments and data handling was provided by a Hewlett-Packard Model 9825 desktop computer.

Typically, cells were first discharged through a 2 Ω resistor for 1 day ($C/20$ rate, *i e*, ~600 mA) then short-circuited for one day, and the impedance was determined (under potentiostatic control) for the totally discharged state (0.0 V d.c. bias) In some cases, impedance measurements were also made at various other states-of-charge, in which case the cell was charged at a current of 600 mA, allowed to equilibrate for about 4 h, and then biased at the voltage yielding zero direct current. Some experiments were performed under galvanostatic rather than potentiostatic control.

Results and discussion

Preliminary studies

Initial studies involved 12 cells, 9 of which had undergone charge/discharge cycling, and were directed toward establishing suitable measurement conditions (charge state, frequency range, integration time, and perturbation magnitude) and baseline data for subsequent comparisons. Cell impedance was measured (under potentiostatic control) using a 10 mV (rms) voltage perturbation for various states of charge, *i e*, totally discharged (0.0 V), slightly charged (1.0 V), and with 4, 8 and 12 A h of charge.

At frequencies greater than about 10 Hz for charged cells and 100 Hz for those totally discharged, the impedance is apparently dominated by inductance associated with the electrical leads. This was demonstrated by measuring the impedance of isolated resistors (0.02, 0.05 and 0.1 ohm) chosen to simulate that of the Ni–Cd cells; an inductive response similar to that obtained for the cells was observed. Because of these results, which are in agreement with those reported in the literature [12], the inductive portions of the impedance spectra were ignored and are not discussed here, although inductive portions of the impedance are included in Bode plots for completeness.

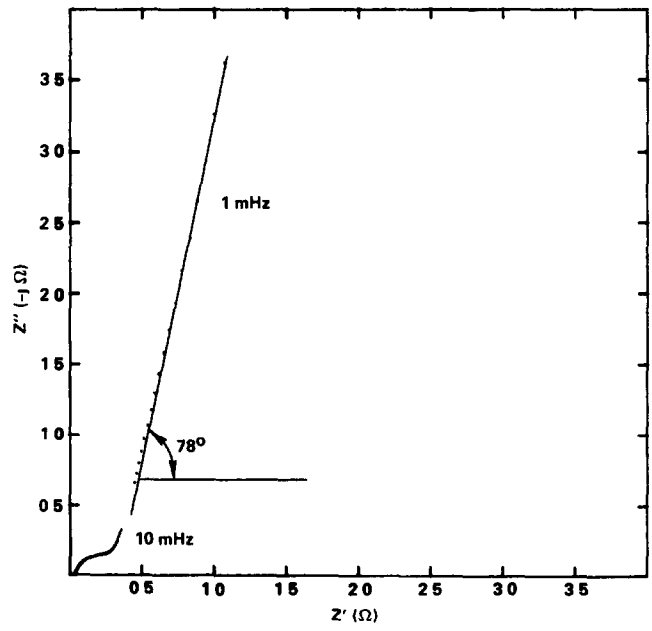

Fig 1 Complex impedance spectrum for Ni–Cd cell L2-92 at 0 0 V (fully discharged)

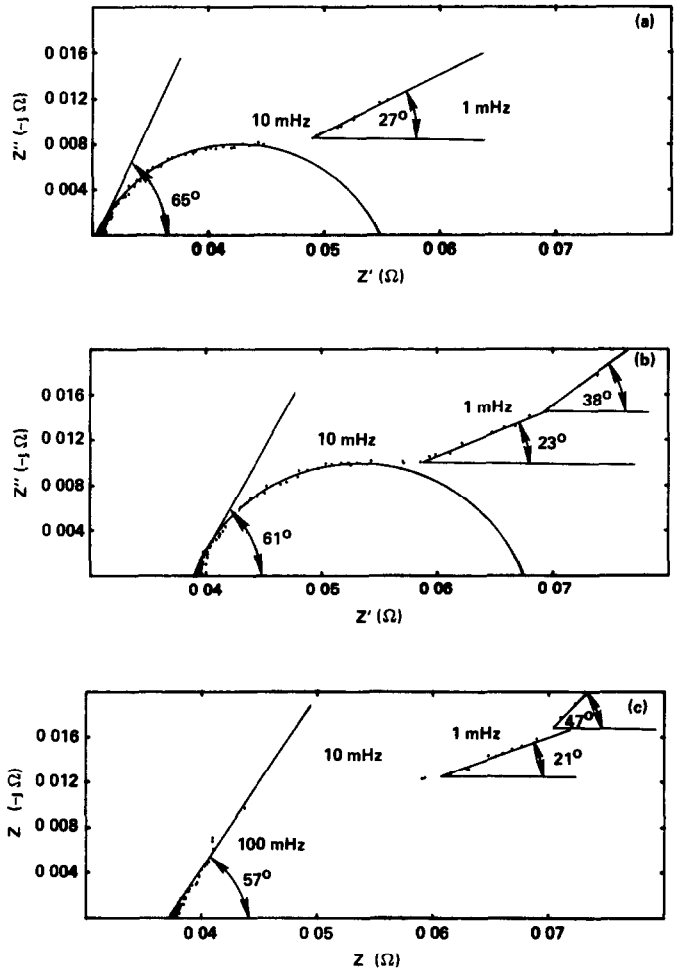

Fig 2 Complex impedance spectra for Ni–Cd cell L2-82 at charge states of (a) 4, (b) 8 and (c) 12 A h

Representative impedance data plotted in the complex plane* for cells at various states-of-charge are shown in Figs. 1 and 2, where Z' and Z'' are the real and imaginary components of the impedance (Z), respectively. In interpreting these data, it is instructive to consider the overall electrode reactions, *i e.*,

$$NiOOH + H_2O + e^- \underset{\text{charge}}{\overset{\text{discharge}}{\rightleftharpoons}} OH^- + Ni(OH)_2 \qquad (1)$$

*Data were plotted in various other ways but only complex plane plots are discussed in this section

$$Cd + 2OH^- \underset{\text{charge}}{\overset{\text{discharge}}{\rightleftharpoons}} 2e^- + Cd(OH)_2 \quad (2)$$

Since Ni–Cd cells are typically constructed with excess negative (Cd) electrode capacity, the cell impedance for the totally discharged state (Fig. 1) is dominated by the fully discharged Ni electrode, in the absence of extraneous factors drastically affecting the reversibility of the Cd electrode. Note that the overall impedance is relatively high, probably because of the presence of a resistive nickel hydroxide layer. In this case the data closely resemble that modelled by the equivalent circuit shown in Fig. 3.

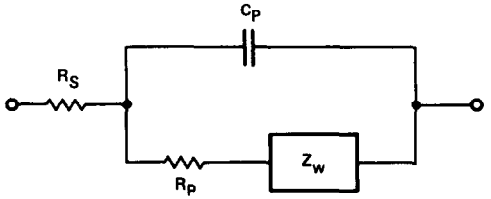

Fig 3 Equivalent circuit for the cell whose impedance characteristics are given in Fig 1

In the frequency range studied, a relaxation process (semicircle defined by R_p and C_p) is observed at frequencies between about 100 Hz and 10 mHz, followed at lower frequencies by a diffusional process (linear region with slope W). The low frequency slopes are considerably greater (65 - 77°) than expected for a diffusional process to either a planar electrode (45°) or an "ideal" porous electrode (22°). Such large slopes are probably associated with a non-ideal pore shape, or with solid-state diffusion or slow adsorption/desorption processes (perhaps involving protons).

For partially or fully charged cells, the impedance behavior is more complex (Fig. 2). Although well-defined semicircles are generally observed for the lower states of charge, the diffusional impedance region is often nonlinear, which makes it difficult to tabulate data and make quantitative comparisons. Nonetheless, the diffusional slopes tend to fall in the range expected for a porous electrode (20 - 40°). Interestingly, for the highest state of charge (12 A h), an inflection in the impedance spectrum is often observed at a value of about 0.042 Ω (see Fig. 2).

In order to draw correlations between impedance characteristics and cycle history and to maximize the probability of including cells that would fail prematurely, emphasis was placed on analyzing the maximum number of cells at only one charge state. The fully discharged state, for which a relatively simple equivalent circuit model appears to be applicable, was chosen. This choice also facilitates data acquisition since the zero charge state can be reproducibly attained, and measurement problems associated with high current response are minimized (cell resistance is largest). In order to minimize the magnitude of the current response at the higher frequencies while

retaining good resolution at the lower frequencies, a perturbation voltage of 2 mV (rms) was selected for subsequent experiments

Failure prediction

Impedance spectra were determined for Ni–Cd cells (in the fully discharged state) at various points during charge/discharge cycle testing and were routinely plotted in the four ways illustrated in Figs. 4 - 7. From the complex plane plots (Fig. 4), R_p, C_p and W were determined (whenever possible) and tabulated*. Log–log (Bode) plots of the total impedance (Z) and its imaginary (Z'') and real (Z') components *vs* frequency (ω) generally exhibited two linear regions (neglecting inductive portions). The slopes and inflection points for such plots were also tabulated, using the notation given in Figs. 5 - 7.

Data for the impedance parameters found to depend on the cell charge/discharge history, *i e*, W and C_p, are summarized in Table 1. For both types of cells (Ni active material chemically deposited for L2 series and electrodeposited for L1 series), W increases steadily with the number of charge/

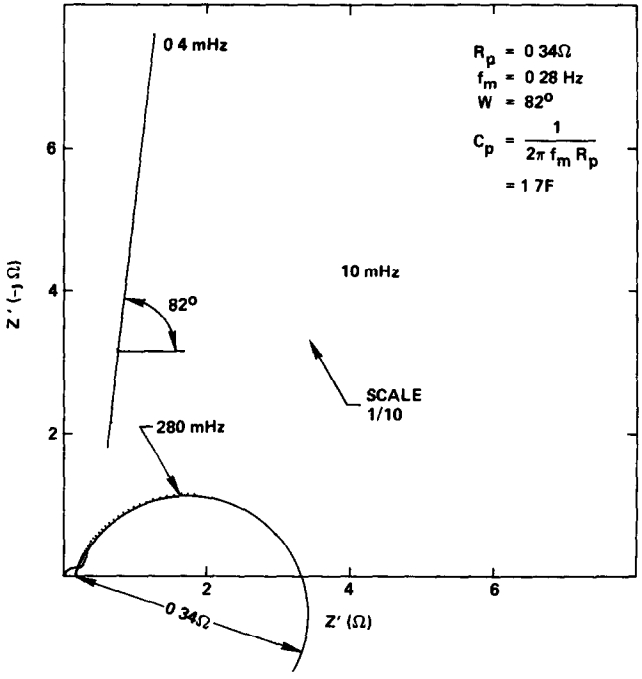

Fig 4 Complex impedance spectrum for Ni–Cd cell L2-59 at 0 0 V after 3457 charge/discharge cycles

*Note that R_s was neglected since it was found to be insensitive to the battery charge state and cycle history

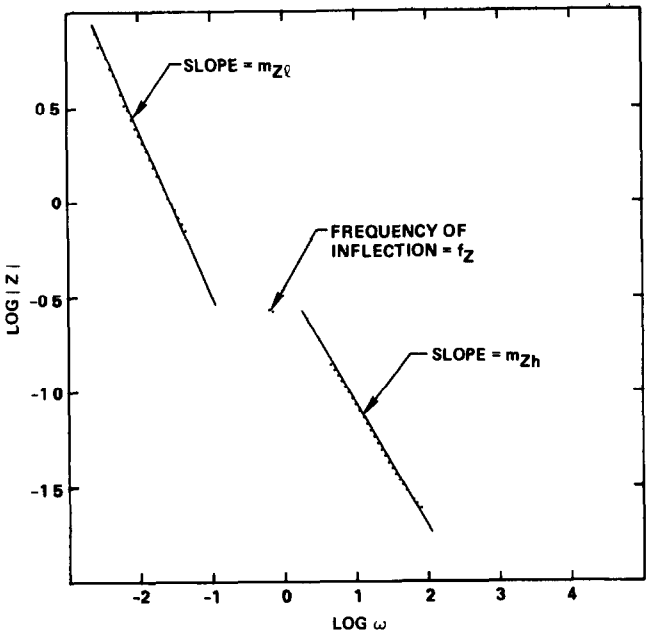

Fig 5 Bode plot of total impedance *vs* frequency for the data given in Fig 4

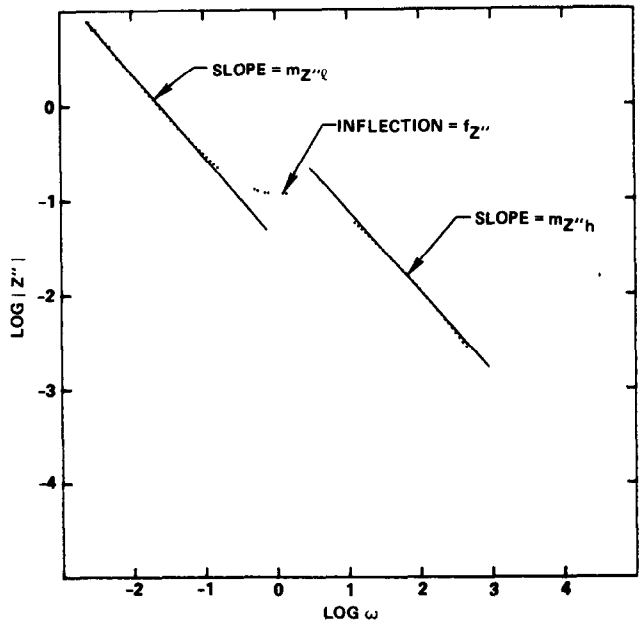

Fig 6 Bode plot of the imaginary impedance component *vs.* frequency for the data given in Fig 4

TABLE 1

Dependence of W and C_p for various Ni–Cd cells on charge/discharge history

Cell no	Cycle temp (°C)	Depth of discharge (%)	Charge/discharge cycles (number)	W (deg)	C_p (F)
L2-59	30	35	1116	76 6	2 2
			3457	82 4	1 7
L2-68	30	20	1957	71 6	—
			3119	77 1	2 1
			4704	78.7	2 0
			5223	82 1	1 8
				-Failed-	
L2-82	40	35	1332	65 6	2 0
			2448	67 4	2 2
			4488	68 1	1 7
L2-93	40	50	378	71 6	5 2
			1496	45 0	—
			3072	69 7	2 2
			3573	-Failed-	
L2-95	40	50	3124	87 1	1 8
			3446	-Failed-	
L2-96	40	50	1561	76 6	1 9
			3025	74 5	—
L2-102	30	50	906	69 7	1 8
			5109	79 9	1 9
L1-68	35	30	0	79 5	8 9
			800	80 5	4 7
			2278	81 4	5 1
L1-69	35	30	0	80 5	5 8
			800	65 6	3 4
			2278	76 9	4 3
L1-70	50	40	0	77 4	4 2
			800	76 3	5 8
			2126	-Failed-	
L1-71	50	40	0	80.2	4 2
			800	76 0	5.4

discharge cycles after the initial conditioning period*. Interestingly, C_p decreases with cycling for L2 cells but increases for L1 cells.

Based on data for two cells, a high or rapidly increasing value for W apparently signals imminent cell failure. This is most evident for cell L2-95

*Note that Ni–Cd cells typically must undergo several charge/discharge cycles before normal behavior is obtained

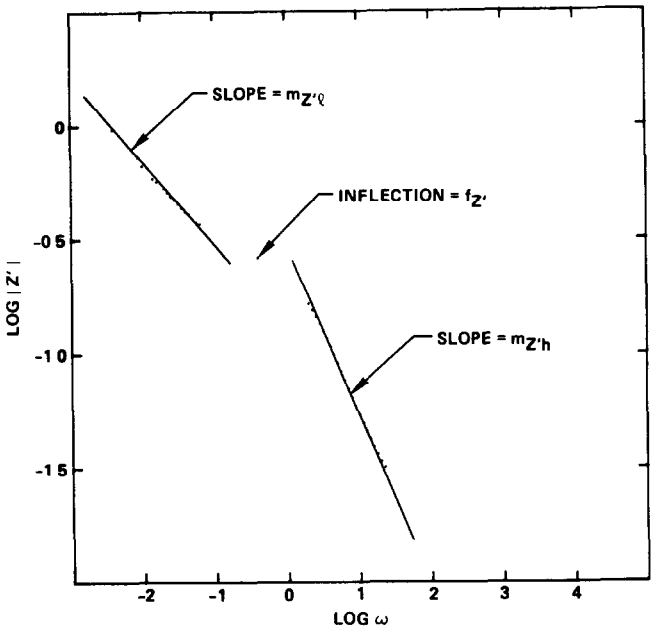

Fig 7 Bode plot of the real impedance component *vs* frequency for the data given in Fig 4

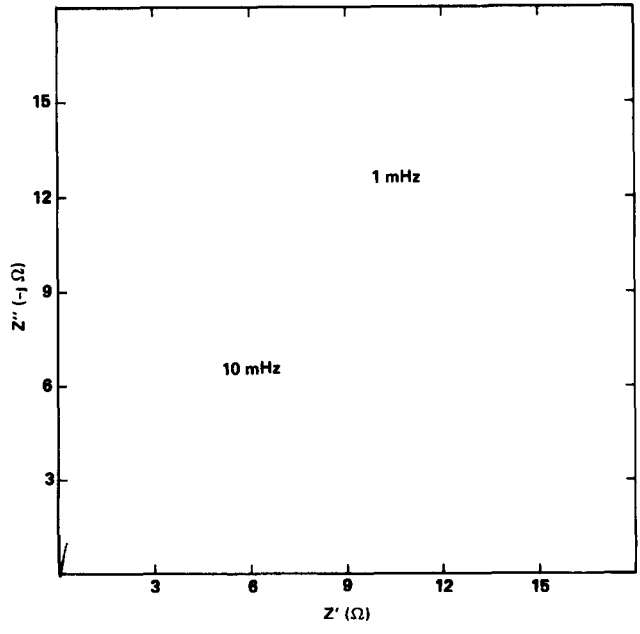

Fig 8 Complex impedance spectrum for Ni–Cd cell L2-95 at 0 0 V after 3124 charge/discharge cycles

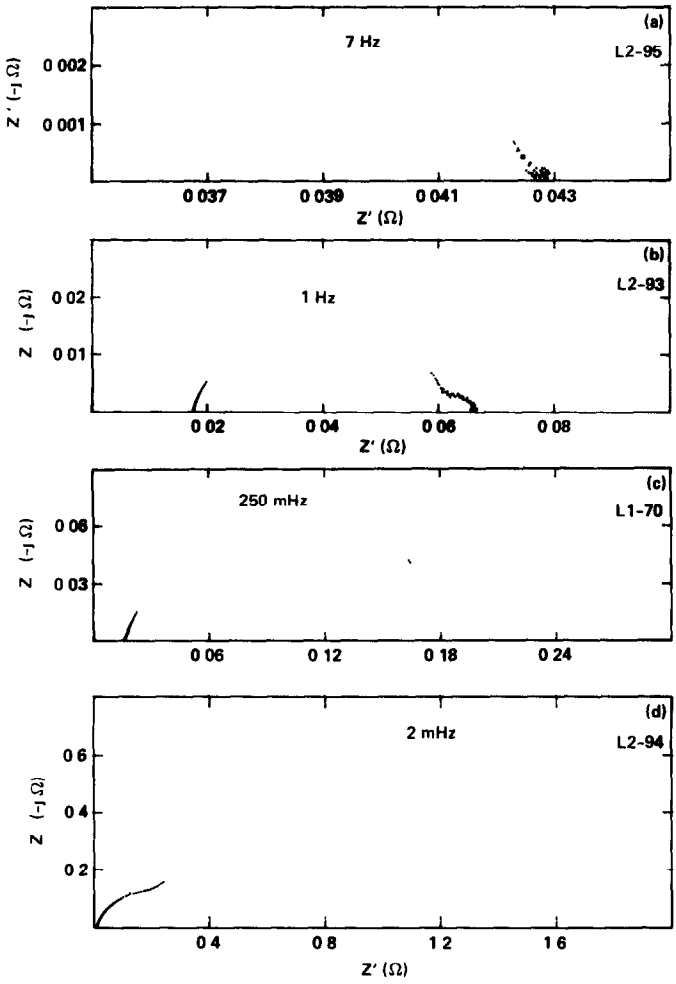

Fig 9 Complex impedance spectra at 0 0 V for failed Ni–Cd cells (a) L2-95, (b) L2-93, (c) L1-70, (d) L2-94

which yielded a W value of 87.1° when evaluated at 3124 cycles (Table 1) and failed only 322 cycles later, note that W typically falls in the 60 - 75° range. The complex impedance spectrum for this cell is shown in Fig. 8. Likewise, W for cell L2-68 steadily increased and was high (82.1°) when evaluated at 5223 cycles, just before failure. Unfortunately, only four of the cells monitored failed during the course of this work so that a firm correlation between W and cell failure could not be established. It should be mentioned, however, that high W values have been reported [7] for Leclanché cells and attributed to polarization of the carbon electrode caused by inadequate sorptive or electrocatalytic properties.

A roll-over of W in the diffusional region may also signal cell deterioration, most probably by a different mechanism. This is evident from

the complex impedance spectra for failed cells shown in Fig. 9. For the first three spectra, (a) - (c), the low frequency diffusional response is absent, presumably because the cells have been shorted by dendrites/separator failure. For these cells, the impedance behavior is apparently dominated by double layer charging and, in cases where two semicircles are observed (Fig. 9(b), (c)), adsorption processes. The impedance spectrum for cell L2-94 (Fig. 9(d)), which comprises a normal high frequency semicircle and a diffusional tail that becomes nonlinear (falls off) at lower frequencies, is of particular interest The latter behavior is typical of diffusion through a finite diffusion layer and has been observed for Ni–Cd cells [12]. The possibility that the deviation of Z'' from linearity in the diffusion region signals cell deterioration is supported by the preliminary data obtained for cell L2-94. Figure 10 depicts the complex impedance spectrum for this cell after 2350 cycles (1000 cycles before failure). The value of W is lower than for most cells, and the curvature in the diffusional region is greater than that observed for any other cell.

As indicated by the impedance data for L1 cells after 800 charge/discharge cycles summarized in Table 2, C_p may also reflect cell deterioration For the harsher cycle conditions (50 °C, 40% depth of discharge), C_p, which also increases with cycle life for this type of cell, is considerably larger Although no correlation was found between m_{Z1} and cell aging, this parameter does appear to be dependent on cycle conditions, as seen in Table 2

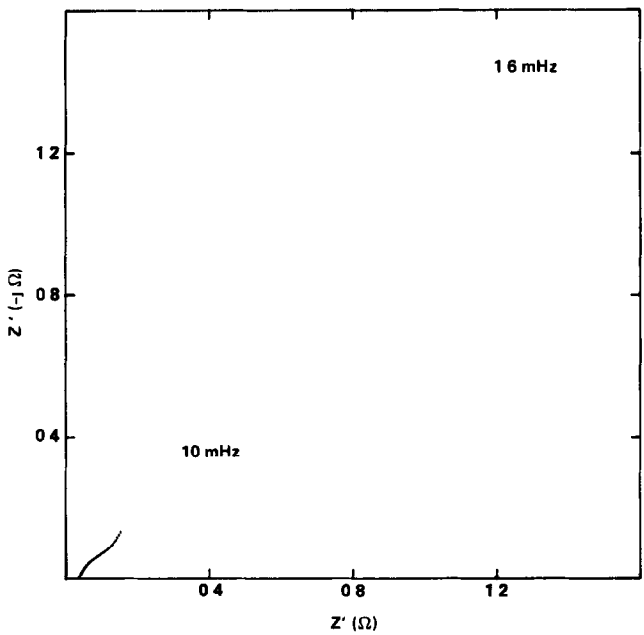

Fig 10 Complex impedance spectrum at 0 0 V for Ni–Cd cell L2-94 after 2350 charge/discharge cycles

TABLE 2

Dependence of C_p and m_{Z1} for L1 cells after 800 charge/discharge cycles

Cell number	Cycle temperature (°C)	Depth of discharge (%)	C_p (F)	m_{Z1}
L1-68	35	30	4 7	−0 96
L1-69	35	30	3.4	−0 92
L1-70	50	40	5 8	−0 86
L1-71	50	40	5 4	−0 75

m_{Z1} = slope of the log Z *vs* log ω plot between ~ 0 4 and 5 mHz

State-of-charge determination

In view of the considerable interest in impedance measurements as a means of determining battery state of charge, data generated under the present program were evaluated for incidental relationships along these lines. It was found that increases in the state of charge are consistently reflected in a linear increase in m_{Zh}, which, as depicted in Fig. 11, is the slope of the linear portion of $\log Z - \log \omega$ plots between about 5 and 500 mHz. Values of m_{Zh} as a function of charge state for 8 Ni–Cd cells are given in Table 3. Although the absolute values vary somewhat, the trend is consistent for each cell. The results indicate that low frequency impedance

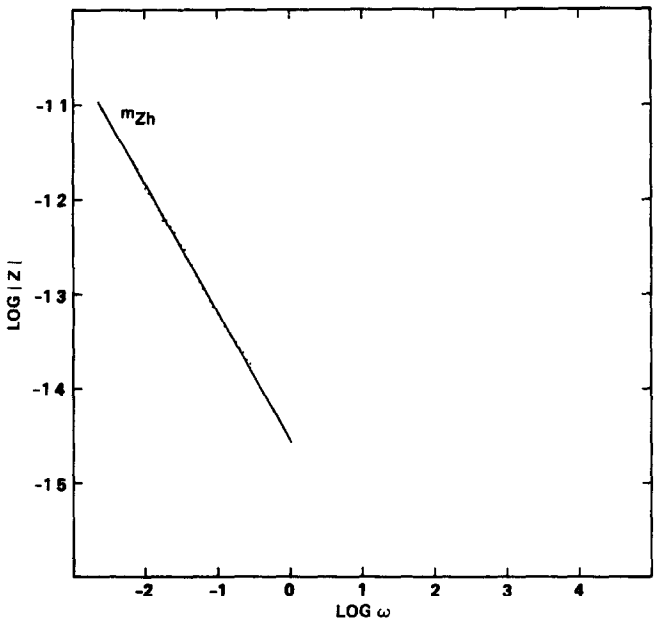

Fig 11 Bode plot of cell impedance *vs* frequency for Ni–Cd cell L2-67 at full charge

TABLE 3

Dependence of m_{Zh} on the charge state of various Ni–Cd cells

State of charge (A h)	m_{Zh}							
	L2-67	L2-72	L2-82	L2-88	L2-92	L2-93	L2-96	L2-102
4	−0 08	−0 062	−0 10	−0 061	−0 083	−0 083	−0 073	−0 10
8	−0 09	−0 069	−0 11	−0 069	−0.080	—	−0 10	—
12	−0 14	−0 095	−0 13	−0 095	−0 095	−0 11	−0 13	−0 18

m_{Zh} = slope of log Z — log ω plot between 500 and 5 mHz

measurements are most promising for state of charge determinations, which is consistent with recent work involving the diffusional impedance for Ni–Cd cells [12].

Conclusions

Impedance characteristics at low frequencies (< 1 Hz) appear to reflect degradation in Ni–Cd cells. Since none of the cells evaluated in the present work failed prematurely (as determined by a failure model proposed by Fedors *et al* [19]) under charge/discharge cycling, it was not possible to establish definite correlations between impedance parameters and cycle life. However, based on the data obtained, such correlations are likely to exist.

Future work in this area should apparently be focussed on the low frequency domain. Since a.c. perturbation measurements are time consuming below frequencies of about 0.001 Hz, alternative measurement techniques should be considered. One possibility is the transient method (described by Pilla [20] and utilized by Zimmerman *et al* [12, 14]), which requires assumptions concerning the natural cell response with respect to background charging or discharging, but which can be performed more rapidly. Another possible approach to reducing measurement time at low frequencies is to use fast Fourier transform (FFT) analysis. In any case, future measurements should probably not be limited to the fully discharged state, for which the nickel electrode dominates the cell impedance, since some important cell failure modes involve the cadmium electrode. For charged or partially charged cells, measurements should be performed galvanostatically so that the overall charge state is not changed during the course of the measurement.

Acknowledgements

The authors express their gratitude to I. Schulman and Ron Baynes of the Jet Propulsion Laboratory for valuable discussions, and Karin Adalian

for assistance in tabulating the data. This work was supported by the National Aeronautics and Space Administration/Jet Propulsion Laboratory under Contract No 955708.

References

1 N A Hampson, S A G. R Karunathilaka and R Leek, *J Appl Electrochem*, *10* (1980) 3
2 S A G R Karunathilaka, N A Hampson, T P Haas, R Leek and T J Sinclair, *J Appl Electrochem*, *11* (1981) 573
3 J J Winter, J T Breslin, R L Ross, H A Leupold and F Rothwarf, *J Electrochem. Soc*, *122* (1975) 1434
4 S A G R Karunathilaka, N A Hampson, R Leek and T J Sinclair, *J Appl Electrochem*, *11* (1981) 365
5 M L Gopikanth and S Sathyanarayana, *J Appl Electrochem*, *9* (1979) 581
6 S A G R Karunathilaka, N A Hampson, R Leek and T J Sinclair, *J Appl. Electrochem*, *10* (1980) 799
7 S A G R Karunathilaka, N A Hampson, R Leek and T J Sinclair, *J Appl Electrochem*, *10* (1980) 603
8 S A G R Karunathilaka, N A Hampson, R Leek and T J Sinclair, *J Appl Electrochem*, *10* (1980) 357
9 M L Gopikanth and S Sathyanarayana, *J Appl Electrochem*, *9* (1979) 369
10 M Keddam, Z Stoynov and H Takenouti, *J Appl Electrochem*, *7* (1977) 539
11 M R Martinelli and A H Zimmerman, Impedance measurements on sealed lead–acid cells, *Aerospace Rep No ATR-78(8114)-1*, The Aerospace Corp, El Segundo, CA, 1978
12 A H Zimmerman, M R Martinelli, M C Janecki and C C Badcock, *J Electrochem Soc*, *129* (1982) 289
13 S Sathyanarayana, S Venugopalan and M L Gopikanth, *J Appl Electrochem*, *9* (1979) 125
14 A H Zimmerman and M C Janecki, in R G Gunther and S. Gross (eds), *Proc Symp on the Nickel Electrode*, The Electrochemical Society, Pennington, NJ, Vol 82-4, 1982, p 199
15 J A Harrison and C E Small, *Electrochim Acta*, *26* (1981) 1555
16 R D Armstrong, K Edmonson and J A Lee, *J Electroanal Chem*, *63* (1975) 287
17 R de Levie, in P Delahay (ed), *Adv Electrochem Electrochem Eng*, Vol 6, Interscience, New York, 1967, p 329 - 397
18 H Keiser, K D Beccu and M A Gutjahr, *Electrochim Acta*, *21* (1976) 539
19 R F Fedors, M Cizmecioglu, S D Hong, A Gupta and J Moacanin, *J Power Sources*, *8* (1982) 369
20 A A Pilla, *J Electrochem Soc*, *117* (1970) 467